Spectroscopy and Optical Maser Action in $SrF_2:Sm^{2+}$

P. P. SOROKIN, M. J. STEVENSON, J. R. LANKARD, AND G. D. PETTIT
Thomas J. Watson Research Center, International Business Machines Corporation, Yorktown Heights, New York
(Received March 9, 1962)

A crystal of $SrF_2:Sm^{2+}$ was operated as a pulsed optical maser at temperatures close to 4.2°K. The 6969 Å output corresponds to the wavelength of an exceedingly sharp line ($\Delta\nu<0.6$ cm^{-1}) in which almost all of the low-temperature fluorescence is concentrated. In contrast to what prevails in $CaF_2:Sm^{+2}$ masers, the output is characterized by strong relaxation oscillations. This may be explained by the large difference in the fluorescent lifetimes in the two systems. While in $CaF_2:Sm^{2+}$ the value of τ is approximately 1.5×10^{-6} sec, in $SrF_2:Sm^{2+}$ it has a value of 15 msec. The reason for the large difference in τ values, in turn, depends upon the relative proximity of the long-wavelength edge of the red band to the position of the metastable $^5D_0$ level from which fluorescence occurs. Absorption measurements taken at helium temperatures on $SrF_2:Sm^{2+}$ show that the lowest vibrational level of the lowest lying $4f-5d$ band lies $\sim$600 cm^{-1} above the position of the $^5D_0$ level while in $CaF_2:Sm^{2+}$ there is near coincidence of the corresponding levels and consequently strong configurational mixing. Crystals of $SrCl_2:Sm^{2+}$ were also studied in this regard and display an expected close similarity in spectral characteristics to $SrF_2:Sm^{2+}$. The vibrational structure on the $4f-5d$ bands is much more pronounced, however, than in $CaF_2:Sm^{2+}$ and $SrF_2:Sm^{2+}$, indicating weaker coupling to the lattice in the excited $5d$ state. A tentative interpretation for the splitting of the red band seen in the absorption spectra of Sm^{2+} ions is given.

INTRODUCTION

THE characteristics of optical masers using the system $CaF_2:Sm^{2+}$ have been recently discussed.[1,2] Among the more interesting features which distinguish this system from other solid state optical maser materials is the short lifetime (1.4×10^{-6} sec) of the maser transition. To this fact is attributed, for example, the absence of "spikes" in the output of the maser when it is pulsed with exciting light. According to the simplest theory of the spike phenomenon originally proposed by Statz and DeMars[3] in connection with microwave masers but more recently reapplied to the optical maser case (numerous references are cited in Sorokin and Stevenson[4]), the number of photons in a coherently excited mode should oscillate violently about the equilibrium number for a time that is no longer than 2τ, where τ is the lifetime of the maser transition, assuming a uniformly-applied pumping pulse. Furthermore, the frequency of these oscillations is also markedly dependent on lifetime, and when one substitutes the known parameters which apply in the case of $CaF_2:Sm^{2+}$ into this theory it appears that the spikes are closely spaced and of such a transient nature that they should not be observed with the resolution of an ordinary photomultiplier system. A simple form of this argument appears in the Appendix.

The short lifetime of the maser transition in $CaF_2:Sm^{2+}$ had been attributed[2,4] to the proximity of the long-wavelength edge of the lowest heavy absorption band to the position of the metastable level from which fluorescence occurs. This fact would allow configurational mixing and result in a partial transfer of intensity from the pumping transitions to the otherwise "forbidden" $4f$-$4f$ maser line. There appears to be general belief that the lowest lying heavy diffuse bands of Sm^{2+}, Eu^{2+}, Yb^{2+}, and Ce^{3+} represent $4f$-$5d$ electric dipole transitions, although $4f$-$6s$ and other possibilities are not excluded. They are certainly not internal $4f$ transitions. Divalent Sm, Eu, and Yb are all easily oxidized to the trivalent state. In these ions the binding energy of the $4f$ electrons is abnormally low until one of them has been excited to a higher level or else completely removed. After this, the nuclear charge can hold the remaining $4f$ electrons firmly enough to prevent the occurrence of quadrivalence. In the case of other rare earths heavy absorption bands usually occur only beyond 50 000 cm^{-1} although in Ce^{3+} they appear at somewhat lower energies than this.

Butement's work[5] shows that the positions of the heavy diffuse bands of the Sm^{2+} ion depend to some extent upon the host lattice into which the ion is incorporated. The positions of the levels from which sharp line fluorescence of the Sm^{2+} ion originates should not, however, change very much with changes in the host lattice since presumably $4f$-$4f$ transitions are here involved and the Sm^{2+} ion is, if anything, better shielded from the effects of the lattice than the $4f$ shell of trivalent rare earth ions. Since Sm^{2+} is isoelectronic with Eu^{3+} the quantum number for the metastable state should be $^5D_0$. Dieke and Sarup[6] have recently shown this to be true for Sm^{2+} in $LaCl_3$, where the separation of the $^5D_0$ and $^5D_1$ levels was found to be 1330 cm^{-1}.

In the light of the above remarks it was of interest to find a crystal other than CaF_2 into which the samarium ion could be incorporated in the divalent state and which could be made to exhibit maser action.

[1] P. P. Sorokin and M. J. Stevenson, IBM J. Research and Develop. **5**, 56 (1961).
[2] C. G. B. Garrett, W. Kaiser, and D. L. Wood, Phys. Rev. **123**, 766 (1961).
[3] H. Statz and G. DeMars, in *Quantum Electronics*, edited by C. H. Townes (Columbia University Press, New York, 1960).
[4] P. P. Sorokin and M. J. Stevenson, in *Advances in Quantum Electronics*, edited by J. Singer (Columbia University Press, New York, 1961).
[5] F. D. S. Butement, Trans. Faraday Soc. **44**, 617 (1948).
[6] G. H. Dieke and R. Sarup, J. Chem. Phys. **36**, 371 (1962).

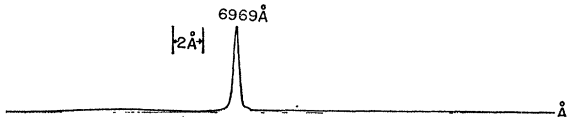

FIG. 1. Fluorescence of $SrF_2:Sm^{2+}$ at near liquid helium temperatures taken with a medium resolution instrument. Signal-to-noise ratio was essentially the same in original trace. Wavelength decreases going from left to right.

$SrF_2:Sm^{2+}$ is such a system and this paper will describe the results of optical maser and spectroscopy measurements made on this system. Also included are the results of some spectroscopic measurements on related systems which have a bearing on the discussion.

FLUORESCENCE ABSORPTION, AND LIFETIME MEASUREMENTS—PRINCIPAL RESULTS

As in the case of $CaF_2:Sm^{2+}$ the fluorescence at near helium temperatures of $SrF_2:Sm^{2+}$ is primarily concentrated in a single sharp line. This line is centered at 6969 Å and at first glance would appear to be the analog of the sharp line in the former system which occurs at 7082 Å. Figure 1 shows a trace of the fluorescence made at a temperature close to that of liquid helium. A Jarrell-Ash 0.5-m scanning spectrometer with 25-μ slitwidths was used for this trace. The lock-in amplifier was set at a relatively low gain. In Fig. 1, there is evident a much weaker broad-band fluorescence at wavelengths slightly longer than that of the principal line; the peak of this extra fluorescence occurs in the vicinity of 6983 Å. There is also present a weak background tapering off very gradually to zero at shorter wavelengths; this is less noticeable in Fig. 1, but shows easily in traces made with a higher lock-in gain. Also there are weak transitions between other multiplets not shown in Fig. 1. All contributions to the fluorescence considered, it appears that at least 50% of the fluorescence is concentrated in the sharp line. From an optical maser viewpoint this is desirable.

The lifetime at near liquid helium temperatures was measured to be approximately 14 msec. This is greater by a factor of 10^4 than the lifetime of the maser transition in $CaF_2:Sm^{2+}$. As a result of this long lifetime, the maser output of $SrF_2:Sm^{2+}$ is characterized by well-defined relaxation oscillations and a long induction time as will be discussed below.

To determine the exact linewidth of the 6969 Å line a special run was made using a Jarrell-Ash 1-m scanning spectrometer in which was installed a Harrison grating. With the slits set at 30 μ the resolution of the instrument should have been 0.2 Å for the 6969 Å line, viewed in eighth order. Under these conditions the trace of Fig. 2 was obtained. There are evident two sidebands of reduced intensity on either side of the central line. The one at shorter wavelengths shows also in Fig. 1. Their origin is not clear. The central line itself is about 0.33 Å wide (approx 0.6 cm^{-1}). Further reduction in slit widths to resolve possible structure in the central line arising from isotope shifts was made difficult by singal-to-noise problems.

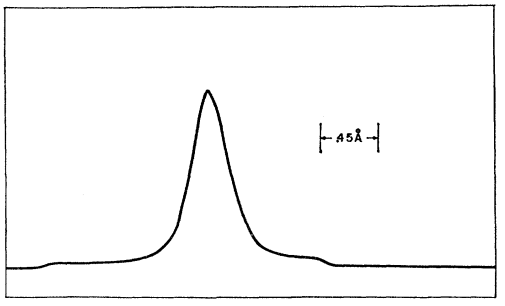

FIG. 2. Fluorescence of $SrF_2:Sm^{2+}$ at near liquid helium temperatures taken with a higher resolution instrument. Signal-to-noise ratio was poorer in original trace. Wavelength decreases going from left to right.

The absorption spectrum at liquid helium temperature is shown in Fig. 3. Its general features are similar to those seen in the absorption spectrum of $CaF_2:Sm^{2+}$ in Fig. 1 of reference 2. In each case there are two main bands in the visible, one occurring in the red and the other centered near 4200 Å. The red band in $SrF_2:Sm^{2+}$ is shifted slightly towards shorter wavelengths in comparison with $CaF_2:Sm^{2+}$. This makes crystals of $SrF_2:Sm^{2+}$ appear blue rather than green when viewed in natural light. In both systems the red band is split into two main components, the longer wavelength one having a smaller absorption coefficient. In both systems pronounced fine structure is present on all main bands. This is probably of vibrational origin as will be discussed below. Correspondence in the two systems can be seen for many of the fine structure lines which appear. In Table I are listed the positions of the longest wavelength lines in the two systems. The two lines in each row correspond to each other in the two spectra.

The sharp lines in the vicinity of 4000 Å are due to trivalent samarium and are also seen in poorly reduced samples of $CaF_2:Sm^{2+}$ as noted by the authors of reference 2. All the remaining absorption is probably due to the divalent ions.

DISCUSSION OF SPECTROSCOPIC RESULTS

The strong absorption line in $SrF_2:Sm^{2+}$ at the long-wavelength "edge" of the red band occurs at 6588 Å (15 177 cm^{-1}). In $CaF_2:Sm^{2+}$ the analogous transition occurs at 6903 Å (14 487 cm^{-1}). This shift of almost 700 cm^{-1} seems large for a transition ($7F_0 \rightarrow 5D_1$) that had been supposed to be wholly within the $4f$ shell.[2] Because of this fact it seems reasonable to assume that the absorption line at 6588 Å in $SrF_2:Sm^{2+}$ as well as the line at 6903 Å in $CaF_2:Sm^{2+}$ arise from transitons

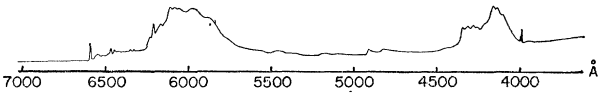

FIG. 3. Absorption spectrum of $SrF_2:Sm^{2+}$ at 5°K.

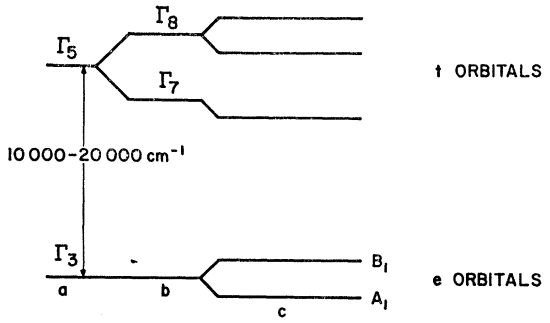

FIG. 4. Term splittings of a single d electron in a cubal and axial field. (a) Levels in a cubal field; (b) levels in a cubal field plus spin-orbit coupling; (c) levels in a cubal field with axial field and spin-orbit coupling of the same order of magnitude. $V_c \gg V_t \sim V_{s.o.}$

from the $7F_0$ ground state to the lowest vibrational level of an excited state. In this excited state, an electron is most likely in a $5d$ state, as mentioned above. Such an electron sees, then, a cubic crystal field with "cubal" symmetry (i.e., anions at the corners of the surrounding cube). In cubal coordination, as opposed to octahedral coordination, the energy of an e orbital is below that of a t orbital. The term splittings for a single d electron in a cubal and axial field are shown in Fig. 4.

Quantum absorption in the Sm^{2+} red band probably corresponds to raising an electron from the $4f$ shell into an e orbital. It might be then thought that absorption in the blue band raises electrons from the ground state to the t orbitals. This, however, is not in accordance with the following observation. Because the energy difference between e and t orbitals is proportional to the crystal field and should vary approximately as $1/R^5$, where R is the distance from the cation to the anion charges, the spacing between the peaks of the red and blue absorption bands should show successive and sizable decreases when the Sm^{2+} ion is placed in CaF_2, SrF_2, and BaF_2, respectively. This does not appear to be the case. At room temperature the red and blue absorption

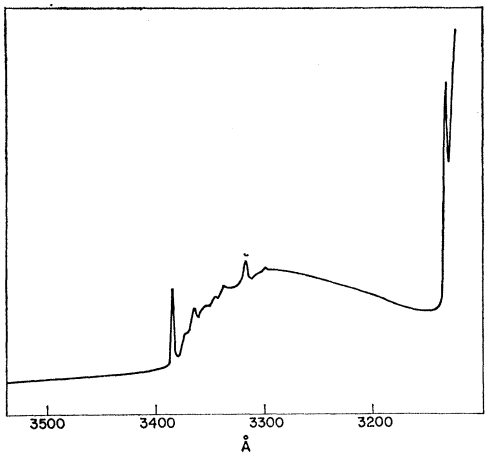

FIG. 5. Absorption spectrum of $CaF_2:Ce^{3+}$ at 5°K.

TABLE I. Longest wavelength lines appearing in absorption in $CaF_2:Sm^{2+}$ and $SrF_2:Sm^{2+}$.

$CaF_2:Sm^{2+}$		$SrF_2:Sm^{2+}$	
(Å)	(cm^{-1})	(Å)	(cm^{-1})
6903	14 487	6588	15 177
6824	14 651	6541	15 288
6777	14 755	6513	15 354
6748	14 819	6465	15 467
6728	14 860	6443	15 521
6664	15 000	6413	15 594
6625	15 095	6388	15 653
6597	15 157	6344	15 762
6576	15 210	6326	15 810
6500	15 384	6225	16 064
6477	15 440	6205	16 116

bands, have maxima at 6200, 4250, 5925, 4128 Å; 6050, 4200 Å in the respective systems. The corresponding energy differences are 7400, 7348, 7281 cm^{-1} and are therefore essentially the same. This energy difference, moreover, is somewhat on the low side of theoretical estimates for the energy difference between e and t orbitals. Leaving unsolved the question of the interpretation of the blue band, we note that the observed splitting of the red band suggests that a Jahn-Teller type of distortion occurs for an excited Sm^{2+} ion. The crystal field symmetry seen by a $5d$ electron in an e orbital may be distorted to tetragonal symmetry, for example, by a small displacement of the excited samarium ion in a [100] direction. Then as Fig. 4 shows, the degeneracy of the e orbital is removed. The driving force for such a distortion would be determined both by changes in the crystal field potential energy accomplished through the distortion and by the spin-orbit interaction. The splitting of the e orbitals in alkaline earth fluoride lattices, if this interpretation is correct, is easily measured from the absorption spectra. For example, at liquid helium temperatures the lowest lying absorption bands of Ce^{3+} in CaF_2 reveal a similar type of splitting to that seen for Sm^{2+} (Fig. 5). The energy difference between the lowest vibrational levels of the split bands is easily measured by inspection. It is approximately 2400 cm^{-1} for Ce^{3+} whereas in $CaF_2:Sm^{2+}$ it is approximately 930 cm^{-1} and in $SrF_2:Sm^{2+}$ it is approximately 910 cm^{-1}. A different value might be expected in the case of Ce^{3+} ions because the $5d$ electron radius is different, corresponding to a more positive

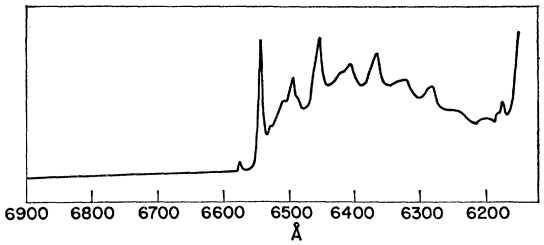

FIG. 6. Absorption spectrum of $SrCl_2:Sm^{2+}$ at 5°K.

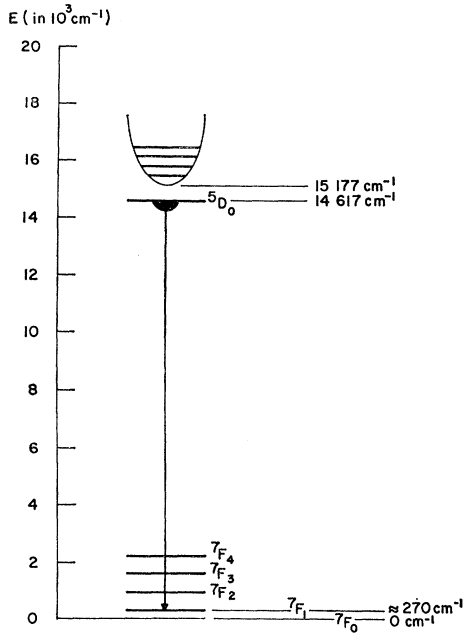

FIG. 7. Energy level diagram for $SrF_2:Sm^{2+}$ showing relative positions of pumping band edge, metastable level, terminal and ground states.

nuclear charge. A more probable explanation for the larger Ce^{3+} splitting is that the crystal field is tetragonal to start with because of the presence of a charge compensating F^- ion in an adjacent [100] site.

The fine structure appearing on the red absorption bands appears to be of vibrational origin. A prominent interval of about 292 cm^{-1} appears in $SrF_2:Sm^{2+}$. The corresponding interval in $CaF_2:Sm^{+2}$ is about 335 cm^{-1}. Figure 6 shows the appearance of the split red band in $SrCl_2:Sm^{2+}$, a system which has the same crystal structure as the $SrF_2:Sm^{+2}$, $CaF_2:Sm^{2+}$ systems. Here the vibrational character of the fine structure is strongly emphasized and the prominent interval is 213 ± 2 cm^{-1}. It is of interest that this interval of 213 cm^{-1} is close to the value 215 cm^{-1} reported by Freed and Katcoff[7] as being prominently seen in absorption in $SrCl_2:Eu^{2+}$ crystals. This fact could be expected if the excited states for both ions were basically the same (i.e., $5d$ orbitals in the same crystal fields).

For Sm^{2+} in SrF_2, then, the appropriate energy level diagram would appear to be as indicated in Fig. 7. The positions of the ^7F multiplet levels are drawn in the positions commonly agreed upon in the works of Butement,[5] Garrett, Kaiser, and Wood,[2] and Dieke and Sarup.[6] No crystal field splittings are indicated in Fig. 7. The $^7F_1$ level position of the metastable level m is deduced by adding 14 347 cm^{-1} (6970 Å) to the 270 cm^{-1} difference between the $^7F_1$ and $^7F_0$ levels. From Fig. 7 one sees that the $^5D_0$ level lies almost 600 cm^{-1} below the lowest vibrational level of the red band. This fact apparently reduces the extent to which the intensity of the $^5D_0$–$^7F_1$ transition is changed due to near coincidence of this energy with that of the strongly allowed $4f$–$5d$ transitions. In $CaF_2:Sm^{2+}$ the edge of the red band lies only 14 487 cm^{-1} above the ground state and thus "crosses" below the position of the unperturbed $^5D_0$ level. In that system strong mixing effects can reasonably be expected to occur, and this is the basic reason for the large difference in radiative lifetimes in the two systems.

Divalent samarium, by analogy with trivalent europium, probably fluoresces via magnetic dipole transitions. The violation of the selection rule $\Delta S=0$ is probably a result of spin-orbit interaction.[8] This effect is explained, for example, in McClure's article[9] and in Troup's.[10] The spin-orbit coupling term $\sum_i \xi(r_i)\mathbf{L}_i\cdot\mathbf{S}_i$ mixes states with the same J and M_J. Thus, $^5D_0$ perturbs $^7F_0$ and $^5D_1$ perturbs $^7F_1$. Thus the terminal state can be written as

$$\psi^1=\psi^0(^7F_1)-\frac{\langle ^7F_1|\,\xi(r)\mathbf{L}\cdot\mathbf{S}\,|^5D_1\rangle}{E(^5D_1)-E(^7F_1)}\psi^0(^5D_1). \qquad (1)$$

The spin-orbit coupling parameter is listed by McClure for many ions on p. 428 of reference 9. For Sm^{2+} one obtains from this table ξ approximately 1100 cm^{-1}. Since the square of the mixing coefficient determines the transition probabilities one has, in terms of f numbers

$$f_{ab}=f^0\left(\frac{k\xi}{E_a-E_b}\right)^2,$$

where f^0 is the oscillator strength of an allowed transition between states of the same multiplicity (here $^5D_1\rightarrow{}^5D_0$). As E_a-E_b equals approximately 14 000 cm^{-1}, f_{ab} should be down from f^0 by approximately a factor of 100 and the lifetime should be correspondingly 100 times longer. For $^5D_1\leftrightarrow{}^5D_0$ the matrix elements are essentially the same as for a free spin transition[10] whose radiative lifetime τ is about 10^{-2} sec at 0.7 μ.

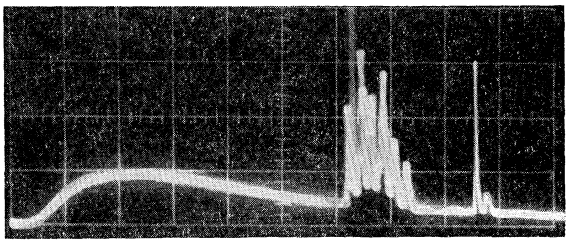

FIG. 8. Pulsed output of $SrF_2:Sm^{2+}$ maser. Sweep rate equals 200 μsec/cm.

[7] S. Freed and S. Katcoff, Physica **14**, 17 (1948).

[8] We are indebted to Dr. John Axe of Johns Hopkins University for pointing out this explanation to us.

[9] D. S. McClure, in *Solid State Physics*, edited by F. Seitz and D. Turnbull (Academic Press Inc., New York, 1959), Vol. 9, p. 427.

[10] G. J. Troup, in *Advances in Quantum Electronics*, edited by J. Singer (Columbia University Press, New York, 1961).

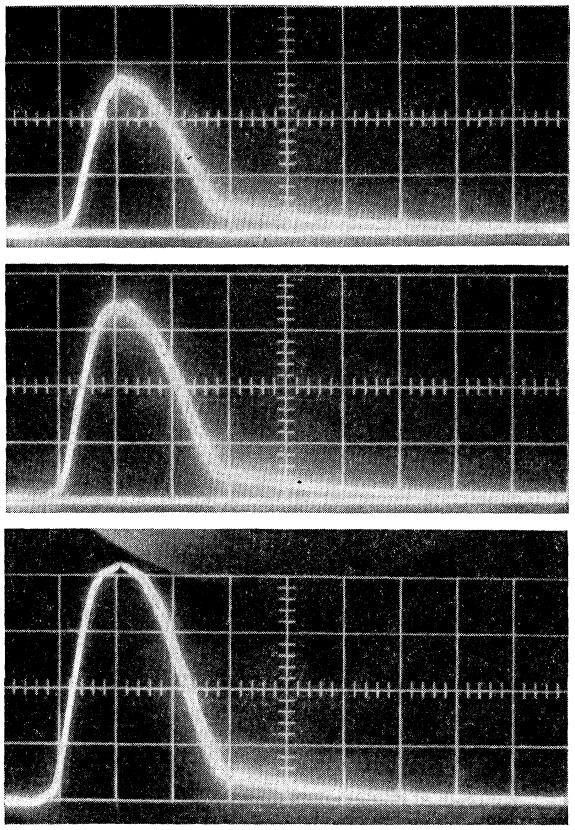

FIG. 9. Pulsed output of $CaF_2:Sm^{2+}$ maser at three pump power levels. Sweep rate equals 200 μsec/cm.

The fact that τ_{obs} is approximately this and not one hundred times greater indicates that perturbing effects of the higher bands are still present in $SrF_2:Sm^{2+}$, though much weaker than in $CaF_2:Sm^{2+}$.

OPTICAL MASER ACTION IN $SrF_2:Sm^{2+}$

A cylindrical crystal of $SrF_2:Sm^{2+}$ with a nominal concentration of 0.1 mole percent samarium was grown for us by Optovac, Inc. The ends were ground flat to one-twentieth of a sodium wavelength and parallel to 15 sec of arc, and were then silvered leaving a 1% transmission on one end. The crystal was mounted in the low-temperature Dewar arrangement described in reference 4. Liquid helium was used as the coolant. Upon excitation above a certain threshold with a pulsed xenon FT524 flash lamp stimulated emission occurred at 6969 Å. A typical trace is shown in Fig. 8. In this particular trace four 100 μF condensers were used and the lamp was set a few inches from the Dewar window. The smooth base pulse seen in Fig. 8 is the pump light. The maser output is characterized by sharp spikes and by a long induction time. Both these features are typical for materials with long radiative lifetimes. For optical masers the population inversion required at threshold is proportional to the lifetime τ and $SrF_2:Sm^{2+}$ thus requires a fairly strong "priming" pulse before oscillation can occur. Once the critical inversion is reached, however, the pumping flux required to sustain oscillation, a quantity generally independent of the lifetime τ, is relatively low in this system because of favorable factors such as the narrow linewidth and apparently high quantum efficiency. From Fig. 8 it is clearly evident that the maser begins to oscillate well after the lamp pulse has passed its maximum and continues to oscillate fairly far out on the tail of the lamp pulse. The $SrF_2:Sm^{2+}$ system is a fairly good candidate for a visible c.w. maser, although it requires temperatures well below that of liquid nitrogen.

COMPARISON WITH MASER OUTPUT OF $CaF_2:Sm^{2+}$

To emphasize the difference between the maser output of $SrF_2:Sm^{2+}$ and $CaF_2:Sm^{2+}$, we have included Figs. 9 and 10 which show some traces of the photomultiplier response to the output from the latter system. The time scale in Fig. 9 is the same as that of Fig. 8. Note the complete absence of spikes, the comparatively early instant at which oscillation starts, and the characteristic feature noted previously[1,2] in $CaF_2:Sm^{2+}$ of the maser shutting itself off at higher pump light levels than required to start oscillation. This last feature has been attributed to heating effects.[2] It is absent in the $SrF_2:Sm^{+2}$ traces. In Figs. 8–10 exactly the same photomultiplier detecting circuit was used. The $CaF_2:Sm^{2+}$ crystal used for the traces of Figs. 9 and 10 was an exceptionally well grown scatter and strain-free crystal prepared for us by J. Scardefield of IBM. Thus an earlier speculation that the spike free nature of the $CaF_2:Sm^{2+}$ maser output might have been due to certain strong mode coupling effects caused by scattering centers in the first samples is apparently ruled out. The explanation for these differences is, as has been emphasized in this paper, found in the Statz-DeMars

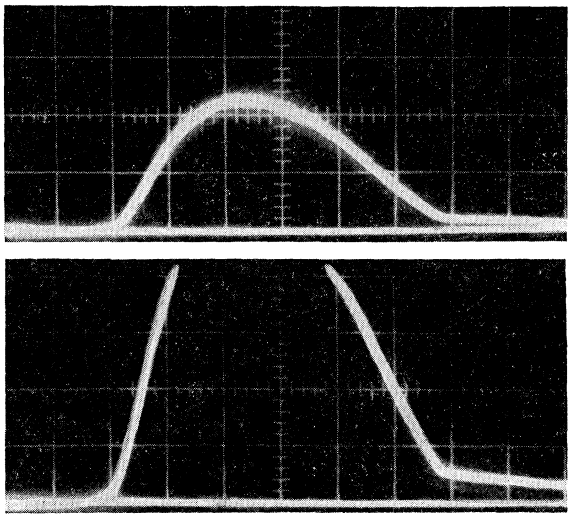

FIG. 10. Pulsed output of $CaF_2:Sm^{2+}$ maser. Sweep rate equals 100 μsec/cm.

theory of relaxation oscillations, a brief version of which appears in the Appendix.

ACKNOWLEDGMENTS

Our thanks are due W. V. Smith and G. Burns for a number of helpful discussions relating to the work reported here. To A. J. Landon we are indebted for much design of the electronic apparatus used with the monochromators to detect and record the fluorescent signals.

We especially wish to thank J. Scardefield for the excellent $CaF_2:Sm^{2+}$ crystal he recently grew for us, traces of whose output are shown in Figs. 9 and 10. Our thanks also extend to W. Hargreaves of Optovac, Inc., for supplying us with the $SrF_2:Sm^{2+}$ crystal. M. Okrasinski and his staff helped us by doing the machine work associated with attachments to the spectroscopic equipment.

APPENDIX

The basic rate equations governing the kinetics of maser action in four level systems are (see references listed in 4)

$$dN/dt=W-NB_sQ-N/\tau, \tag{A1}$$

$$dQ/dt=NB_sQ-Q/t_c+N/p_m\tau. \tag{A2}$$

Here, Q is the number of quanta in the mode in which the coherent oscillation is being built up and N is the number of excited ions in the crystal. The quantity p_m is the number of modes coupled to the fluorescent linewidth and for a Lorentzian line is given by

$$p_m=8\pi^2\nu^2\Delta\nu V/c^3.$$

Since the rate of stimulated emission due to a single quantum in a single mode is just equal to the rate of spontaneous emission into the same single mode,

$$B_s=1/\tau p_m.$$

The decay of photons out of the cavity mode due to reflection losses is represented by the quantity $t_c=Ln_r/c(1-R)$.

Equations (A1) and (A2) are nonlinear in N, Q but approximate solutions are available which represent the asymptotic behavior as the number of excited ions and the number of photons in the coherent field strive to come into equilibrium when a steady pumping source is turned on. What follows is essentially taken from Sec. 5 of reference 2 but is here included because of slight differences in the final formulas. For the small oscillations about the steady state one writes

$$n=N-N_0,$$
$$q=Q-Q_0.$$

Neglecting second-order terms and the term $N/p_m\tau$ in Eq. (A2), one has

$$dn/dt=[W-N_0Q_0B_s-(N_0/\tau)]-n[Q_0B_0+(1/\tau)]-qN_0B_s,$$
$$dq/dt=[N_0Q_0B_s-(Q_0/t_c)]+nQ_0B_s+q[N_0B_s-(1/t_c)].$$

Three of the six right-hand terms are equal to zero by virtue of the steady-state conditions and one is left with the set

$$dn/dt=-n[Q_0B_s+(1/\tau)]-qN_0B_s,$$
$$dq/dt=nQ_0B_s.$$

Then

$$d^2n/dt^2+dn/dt[Q_0B_s+(1/\tau)]+(Q_0B_s/t_c)n=0,$$

and exactly the same equation holds for q. A trial solution is

$$n=n_0e^{-(\alpha-i\omega)t}.$$

Substituting this function into the differential equation and setting real and imaginary parts equal to zero,

$$\alpha=1/2(Q_0B_s+1/\tau),$$
$$\omega=\left(\frac{Q_0B_s}{t_c}-\frac{Q_0^2B_s^2}{4}-\frac{Q_0B_s}{2\tau}-\frac{1}{4\tau^2}\right)^{\frac{1}{2}}.$$

The quantity Q_0B_s may be comparable to $1/\tau$ if the steady state is not very much above the threshold situation. The quantity t_c, however, is less than τ usually, and therefore as one approaches threshold conditions

$$\omega\cong(Q_0B_s/t_c)^{\frac{1}{2}}.$$

Therefore, other factors being equal, ω varies as $(1/\tau)^{\frac{1}{2}}$. For $CaF_2:Sm^{2+}$, ω should be approximately 100 times its value in $SrF_2:Sm^{2+}$. Examination of Fig. 8 shows that a spiking frequency a hundred or so times greater than appears there would be hard to resolve. Also the formula for α shows that the spikes should die away in less than a microsecond for $CaF_2:Sm^{2+}$ but should be only slightly damped for the whole duration of the maser pulse for $SrF_2:Sm^{2+}$.

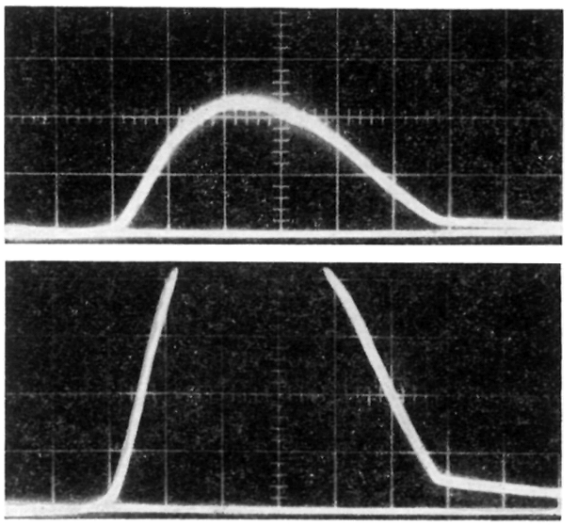

FIG. 10. Pulsed output of $CaF_2:Sm^{2+}$ maser.
Sweep rate equals 100 μsec/cm.

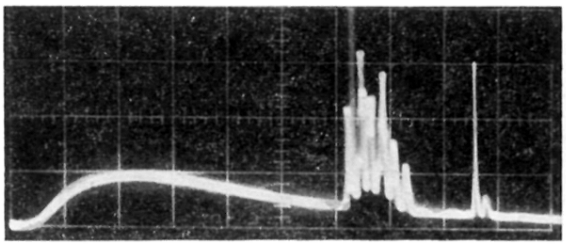

FIG. 8. Pulsed output of $SrF_2:Sm^{2+}$ maser.
Sweep rate equals 200 μsec/cm.

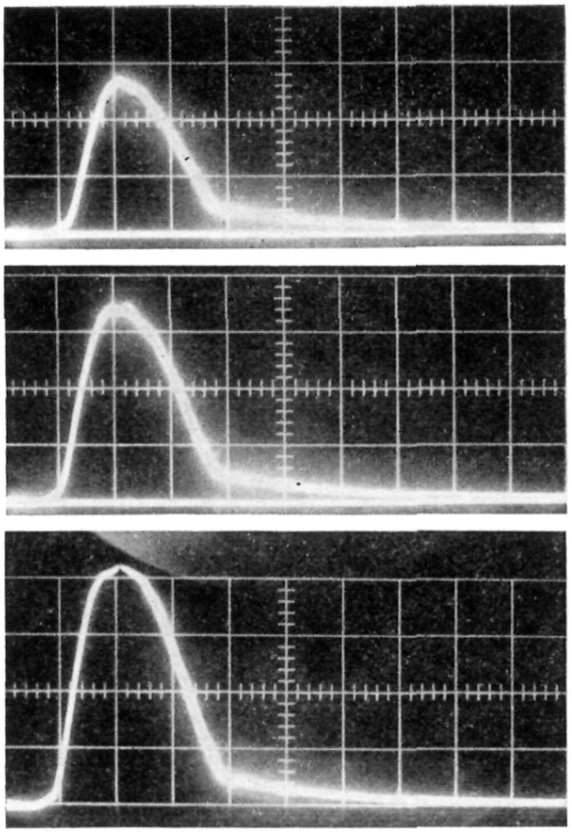

FIG. 9. Pulsed output of $CaF_2:Sm^{2+}$ maser at three pump power levels. Sweep rate equals 200 μsec/cm.